Journal of Materials Chemistry A

Accepted Manuscript

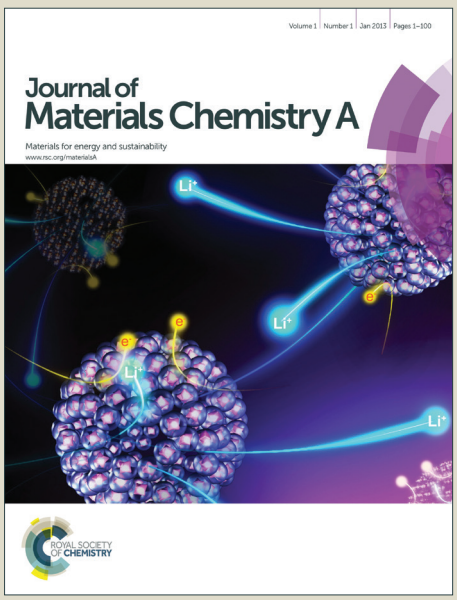

ROYAL SOCIETY OF CHEMISTRY

www.rsc.org/materialsA

Polymer Electrolytes based on Dicationic Polymeric Ionic Liquids: Application in Lithium Metal Batteries

Kun Yin [a], Zhengxi Zhang [a,*], Xiaowei Li [a], Li Yang [a, c ,*], Kazuhiro Tachibana [b], Shin-ichi Hirano [c]

Abstract

Polymeric ionic liquids (PILs) have stirred great interest for their potential application as electrolyte hosts in lithium metal batteries (LMBs) because of their desirable performance. In this work, PIL-based gel polymer electrolytes applied in lithium metal batteries (LMBs) at low-medium temperatures (25℃, 30℃ and 40℃) are firstly reported. A novel imidazolium-tetraalkylammonium-based dicationic polymeric ionic liquid, poly(N,N,N-trimethyl-N-(1-vinlyimidazolium-3-ethyl)-ammonium bis(trifluoromethanesulfonyl) -imide) is successfully synthesized, and its structure and purity are confirmed by ^{1}H NMR, FTIR and elemental analysis. Subsequently, the ternary gel polymer electrolytes are prepared by blending the as-synthesized dicationic PIL as the polymer host with 1,2-dimethyl-3-ethoxyethyl imidazolium bis(trifluoromethanesulfonyl) imide (IM(2o2)11TFSI) ionic liquid and LiTFSI salt in different weight ratios. The PIL-LiTFSI-IM(2o2)11TFSI electrolytes reveal low glass transition temperatures around -54℃ and high thermal stability to about 330℃. Moreover, the ternary gel polymer electrolytes show good ion conductivity around 10^{-4} S cm^{-1} at low-medium temperatures, high electrochemical stability and good interfacial stability with lithium metal. Particularly, the Li/$LiFePO_4$ cells assembled with polymer electrolytes at 0.1C rate are able to deliver discharge capacities of about 160 mAh g^{-1}, 140 mAh g^{-1}and 120 mAh g^{-1} at 40℃, 30℃ and 25℃, respectively, with excellent capacity retention, as well as exhibit acceptable rate capability. These findings reveal that dicationic PIL-based electrolytes have great potential for use as safe electrolytes in LMBs.

1.Introduction

Lithium ion batteries employing lithium metal as a anode electrode, that is, lithium metal batteries (LMBs) are considered as one of the most attractive contenders for the next generation energy storage systems, since metallic lithium can provide the largest specific capacity (~ 3860 mAh g^{-1}), which is about ten times that of the commercially used graphite anode (~ 380 mAh g^{-1}).[1] Despite these desirable features, developing practical LMBs is a challenging task owing to dendrite formation from uneven lithium deposition during successive charge-discharge cycles,[1] which eventually leads to internal short circuits and thermal runway. It has been reported that aprotic organic electrolytes are responsible for this phenomenon to a great extent.[1, 2] Hence, replacing organic electrolytes by novel electrolyte materials that can offer intrinsic safety is on the research frontier in both academia and industry.[3, 4]

Gel polymer electrolytes (GPEs) which use polymer hosts to immobilize liquid electrolytes combine the advantages of polymer materials (avoiding liquid leakage, no separator needed) with those of liquid electrolytes (good electrochemical properties).[5, 6] Furthermore, it has been confirmed that compared to liquid electrolytes, dendrite formation could be suppressed in GPEs because of the immobility of electrolyte molecules.[7-10] In view of these superior properties, GPEs have attracted great attention as promising safe electrolytes in recent years. To date, two types of host polymers are introduced for GPEs preparation. The first one is the conventional polymer materials, including poly(ethylene oxide) (PEO), poly(vinylidene fluoride) (PVdF), poly(methyl methacrylate) (PMMA), poly(acrylonitrile) (PAN) , and co-polymers or blends of these systems.[11-13] However, GPEs based on conventional polymer hosts mentioned above still encounter lack of stability with time due to the leaching of liquid from GPEs.[5, 14] The second species is polymeric ionic liquids (PILs), in which ion species remain covalently bound to the polymer backbone.[15] PILs represent an significant class of materials as they show interesting properties, such as high thermal stability, good film forming ability and chemical compatibility with ionic liquids (ILs).[16, 17] In spite of extensive research about synthesis and properties of PILs over the past decade,[15, 18-24] a few PILs as hosts in GPEs have been applied in LMBs. Appetecchi et al.[25] firstly explored the application of GPEs with the pyrrolidinium-based PIL as the host in LMBs. The Li/$LiFePO_4$

cells at 40℃ can deliver discharge capacity of 144.1 mAh g^{-1} at 0.1C rate. Later, Li et al.[26, 27] prepared GPEs based on guanidinium-based PILs as polymer hosts, and studied their performance in LMBs. It was found that although the Li/$LiFePO_4$ cells export discharge capacities of about 140 mAh g^{-1} at 0.1C rate at a high temperature (80℃), they are not able to permit operation at the decreased temperature. Subsequently, Li et al.[28, 29] further synthesized homo tetraalkylammonium-based PILs as hosts in GPEs, and the Li/$LiFePO_4$ cells containing such GPEs are capable to properly operate at 60℃. Recently, imidazolium-based PIL electrolytes applied in LMBs has been reported by our group,[30] and the cell test revealed that Li/$LiFePO_4$ cells containing GPEs with the imidazolium-based PIL host obtained by the desirable synthetic route can achieve discharge capacity of about 160 mAh g^{-1} at 0.1C rate and 60℃. According to these previous works, we could find that PILs commonly have monocationic center repeat units, i.e., monocationic PILs. Moreover, most of monocationic PIL-based electrolytes applied in LMBs are operated only at/above 60℃, while quite few monocationic PILs-based electrolytes could be performed well in LMBs at 40℃. Whether LMBs assembled with PIL-based electrolytes exhibit satisfactory performance at low-medium temperatures, i.e. from room temperature to 40℃, remains an unanswered issue that must be addressed to promote the practical use of LMBs. In order to respond effectively to this challenge, it is imperative and important to explore PILs with new structures, other than monocationic PILs, as hosts in GPEs.

Inspired by above analysis, in this article, we synthesized a novel dicationic PIL, that is, imidazolium-tetraalkylammonium-based PIL, poly(N,N,N-trimethyl-N-(1-vinlyimidazolium-3-ethyl)-ammonium bis(trifluoromethanesulfonyl) -imide) (poly[VIm][TMEN][TFSI]), as outlined in Fig. 1.(a). At the same time, GPEs with different weight compositions were obtained by incorporating the PIL (poly[VIm][TMEN][TFSI]) as the polymer host, a 1,2-dimethyl-3-ethoxyethyl imidazolium bis(trifluoromethanesulfonyl) imide (IM(2o2)11TFSI) ionic liquid shown in Fig. 1(b) and LiTFSI salt. The thermal and electrochemical properties for as-obtained ternary GPEs were investigated, and their potential application in LMBs at low-medium temperatures (25℃, 30℃ and 40℃) were evaluated.

[Figure 1]

2. Experimental

2. 1. Materials

1-vinylimidazole (VIm) (>98%) was purchased from TCI Chemical. (2-bromoethyl)trimethylammonium bromide (99%) and 1, 2-dimethylimidazole (98%) were purchased from J&K Chemical. 2,2'-azobis(isobutyronitrile) (AIBN) was purchased from Aladdin, and AIBN was recrystallized from ethanol. 2-Bromoethyl ethyl ether (98%) was purchased from Energy Chemical. Lithium bis(trifluoromethylsulfonyl)imide (LiTFSI) was kindly provided by Morita Chemical Industries Co., Ltd. All other reagents, solvents and salts were used as received.

2.2. Synthesis of PVIm homopolymer

The PVIm was synthesized by radical polymerization of 1-vinylimidazole (VIm) in toluene with AIBN as an initiator. The desired amount of VIm monomer was dissolved in toluene, and then the initiator (0.5 wt.% with respect to monomer) was added to the reaction mixture. The reaction mixture was stirred under Ar at 65℃ for 8 h. The polymer was washed with acetone (5x), subsequently filtered, and finally dried in vacuum oven at 75℃ for 24 h.

2.3. Synthesis of bromide intermediate, poly[VIm][TMEN][Br]

Poly[VIm][TMEN][Br] was synthesized by refluxing the mixture of PVIm (1 equiv. with respect to monomer unit) and (2-bromoethyl)trimethylammonium bromide (1.2 equiv) in ethanol solution for 6 days at 75℃. The product would be precipitated from the mixture at the end of the reaction. Then the bromide intermediate was washed with ethanol (3x) at 75℃ under refluxing to remove the unreacted (2-bromoethyl)trimethylammonium bromide. Finally, the as-obtained poly[VIm][TMEN][Br] was dried under high vacuum at 75℃ for 24 h.

2.4. Synthesis of dicationic imidazolium-tetraalkylammonium-*based PIL, poly[VIm][TMEN][TFSI]*

The bromide intermediate, poly[VIm][TMEN][Br] (1 equiv. with respect to monomer unit) was dissolved in deionized water. LiTFSI (1.2 equiv.) was added and the reaction mixtures were stirred for 2 h, and large amounts of white powder precipitated from the solution. After filtration, the white powder was washed with deionized water several times until residual by-product (LiBr) can not be detected with the use of $AgNO_3$ (0.1 M). The solid was dried under

high vacuum at 90℃ for 36 h to yield the resulting poly[VIm][TMEN][TFSI].

2.5. Synthesis of an ionic liquid, 1,2-dimethyl-3-ethoxyethyl imidazolium bis(trifluoromethanesulfonyl) imide (IM(2o2)11TFSI)

IM(2o2)11TFSI was synthesized according to previous report,[31] and its chemical structure was confirmed by ^{1}H NMR spectrum.

2.6. Preparation of gel polymer electrolyte based on PIL, poly[VIm][TMEN][TFSI] as polymer host

The gel polymer electrolytes with three different weight compositions (Table 1) were prepared by dissolving the as-prepared PIL (host), IM(2o2)11TFSI (ionic liquid) and LiTFSI (salt) in acetone. The mixtures were casted into PTFE slides to prepare the electrolyte membranes. Then the GPEs were dried under the protection of Ar atmosphere at room temperature for 16 h, and then, dried under vacuum at 90℃ for 36 h. Finally, the GPEs were moved into an argon-filled glove box (O_2 < 0.1 ppm, H_2O < 0.1 ppm) and dried for 48 h to remove the final traces of acetone. As shown in Fig. 1 (c), the obtained PIL-based polymer electrolytes are self-standing and flexible.

[Table 1]

2.7. Test cells assembly

The CR2016 coin-type cells were set up. The cathode was prepared by mixing $LiFePO_4$, acetylene black and poly(vinylidene fluoride) (PVDF) with a weight ratio of 8:1:1. The active material loading was ca. 1.5-2.5 mg cm^{-2}. Lithium metal foil (battery grade) was used as the anode. The coin-type battery test cells were assembled by laminating a $LiFePO_4$ cathode, a dicationic PIL-based electrolyte membrane and a lithium foil in the argon-filled UNILAB glove box.

2.8. Measurements

The chemical structures of polymers obtained in this work were confirmed by ^{1}H NMR (Avance III 400) technique. Fourier-transform infrared (FT-IR) spectroscopic measurements were recorded on a Bruker IFS-28 FT-IR spectrometer. Elemental composition (C, N, S and H) was measured by an elemental analyzer (Elementar, Vario-ELIII IRMS).

The intrinsic viscosity ([η]) of poly[VIm][TMEN][TFSI] was measured by empolying an Ubbelohde dilution

viscometer at 25℃ in acetone. The value of viscosity-average molecular weight (M_v) of poly[VIm][TMEN][TFSI] was calculated by using the Mark-Houwink-Sakurada equation $[\eta] = KM_v^a$, wherein $K = 6.76\times10^{-3}$ cm^3 g^{-1} and a = 0.71, which were determined in a PMMA/acetone solution at 25℃.[32] The result showed that $[\eta] = 113.9$ cm^3 g^{-1}, and $M_v = 1.13\times10^6$ g mol^{-1}.

The calorimetric measurements were made with a differential scanning calorimeter (DSC, TA Instruments Q2000) in the temperature rang -80℃ to 200℃. The PIL and electrolyte samples (about 15mg) were sealed in aluminum pan, then heated and cooled at scan rate of 10℃ min^{-1} under a flow of nitrogen. The thermal data were collected during heating in the second heating scan. The thermal stabilities were measured with TGA (TA Instruments Q5000) in the temperature range between 40℃ and 600℃, under N_2 atmosphere at a heating rate of 10℃ min^{-1}.

The ionic conductivity of the PIL-LiTFSI-IM(2o2)11TFSI electrolyte membrane was measured by impedance measurements using a CHI660B Electrochemical Workstation. The data were collected over a frequency range 0.1 Hz-100 kHz with amplitude of 5 mV for an open circuit potential from 25 to 90℃. The ionic conductivity (σ) of polymer electrolytes was calculated using the following equation:

$$\sigma=\frac{L}{R\cdot S}$$

Here, R is the bulk electrolyte ohmic resistance, S and L are the area and thickness of the polymer electrolyte film, respectively.

The electrochemical stability of as-prepared dicationic PIL-based electrolytes was evaluated by linear sweep voltammetry (LSV) at 40℃ (scan rate 10 mV s^{-1}) with a CHI660B Electrochemical Workstation. The cells used for this investigation was assembled by sandwiching dicationic PIL-based electrolyte between the stainless steel (SS) and the lithium metal, in which the stainless steel was employed as working electrode and the lithium metal was employed as counter and reference electrodes. Separate tests were performed on each sample for the cathodic and anodic stability measurements by scanning the cell potential from open-circuit voltage to positive (anodic) or negative (cathodic)

voltages.

Symmetric lithium metal coin cells (CR2016 stainless steel cell, 16 mm diameter disc of lithium metal and dicationic PIL-based electrolyte) were assembled in the glove box. After the cells kept at open circuit at 40℃ for 36 h, charge-discharge cycling were measured at CT2001A cell test instrument (LAND Electronic Co., Ltd.) at 40℃ under two current densities, 0.05 mA cm^{-2} and 0.1 mA cm^{-2}, for each polarization (16 min charge and 16 min discharge). Impedance spectroscopy of symmetrical cell was undertaken on CHI660B Electrochemical Workstation (0.1Hz-100kHz, amplitude voltage 5 mV) at 40℃ before and after cycling.

The cycling tests on Li/ PIL-based electrolyte/ $LiFePO_4$ batteries were performed at low-medium temperatures (25℃, 30℃ and 40℃) using a CT2001A cell test instrument (LAND Electronic Co., Ltd.). The discharge current rates were varied from 0.1C to 1C, while the charge current rate was fixed to 0.1C. Constant current charge-discharge cycles were tested between 2.5 and 4.0 V (vs. Li/Li^+).

3.Results and discussion

The dicationic PIL (poly[VIm][TMEN][TFSI]) is synthesized via a three-step process, that is, starting from the radical polymerization of VIm monomer followed by quaternization and anion exchange reactions. The chemical structure and purity of this obtained polymer are characterized by ^1H NMR, FTIR and elemental analysis, as displayed in Fig. 2. Fig. 2(a) shows the ^1H NMR spectrum of poly[VIm][TMEN][TFSI] in DMSO-d6. In this spectrum, the signals corresponding to the polymer backbone protons can be found at around 2.19 and 4.54 ppm, while the signals at 8.95 ppm (1H), 7.74 ppm (1H), and 7.30 ppm (1H) belong to the imidazolium ring protons. Besides, the proton signals of $-CH_2CH_2-$ and $–CH_3$ in side chain can be observed at around 4.54 and 3.49 ppm, respectively. Also, it should be pointed out that the signals at 2.5 ppm and 3.3 ppm correspond to the protons of DMSO-d6 solvent and HDO existing in DMSO-d6, respectively. Fig. 2(b) presents the FT-IR spectrum of poly[VIm][TMEN][TFSI]. The adsorption peaks at 3146 cm^{-1} and 2921 cm^{-1} correspond to the C-H stretching vibration from the imidazole ring and the alkyl chains. The C ＝N and C-N stretching vibration of the imidazole ring are observed at 1632 and 1135 cm^{-1}, respectively.[33] In addition,

the neighbored bands centered at 1488 cm^{-1} can be assigned to the C-N vibration from the tetraalkylammonium cations.[34] The characteristic bands of the $TFSI^-$ anion can be found at 1350, 1195, 1056, 653, and 571 cm^{-1}.[23, 28, 33] According to the analysis of ^1H NMR and FT-IR, it proves the successful formation of the poly[VIm][TMEN][TFSI]. Moreover, the elemental analysis result for poly[VIm][TMEN][TFSI] (Anal. Found: C 23.84, N 9.97, S 16.62, H 2.9. Anal. Calcd.: C 22.67, N 9.44, S 17.39, H 2.58) also confirms high purity.

[Figure 2]

[Figure 3]

The thermal properties of the neat PIL polymer and PIL-based electrolytes were evaluated by DSC (Fig. 3(a)) and TGA (Fig. 3(b)) measurements. As clearly evidenced from Fig. 3(a), the neat PIL polymer only shows a glass transition temperature (T_g) around 106.6℃, indicating an amorphous polymer. According to our previous report,[31] the neat IM(2o2)11TFSI ionic liquid does not exhibit any phase transition behavior until -60℃ during the second heating scan process, thus its melting point can be denoted as <-60℃. Moreover, it can be seen that the addition of the IM(2o2)11TFSI ionic liquid to the PIL polymer could drastically decrease the glass transition temperature. This drop in T_g can be attributed to that the IM(2o2)11TFSI IL as a plasticizer in the electrolytes increases the free volume of the PIL, and further helps the segmental motion of the PIL chains.[35] When the IM(2o2)11TFSI content reaches to 90 wt.%, 95 wt.% and 100 wt.% (with respect to host), the T_g of PIL-based electrolytes reduced to about -52℃, -54℃ and -56℃, respectively. The decrease in T_g with the slight increase of IM(2o2)11TFSI content demonstrates that the glass transition feature of the PIL-based electrolytes would be sensitive with the IM(2o2)11TFSI content change. In addition, no other endothermic peaks are observed in the DSC traces of PIL-based electrolytes, suggesting that a lithium salt/ionic liquid phase separation phenomenon does not occur. This result is similar to the investigation of the previously reported mono-guanidinium based PIL electrolytes containing a guanidinium IL,[26] however, it is different from that reported for mono-pyrrolidinium based PIL electrolytes incorporating a pyrrolidinium IL.[25]

Thermal stability is also an important parameter for evaluating PIL-based electrolytes. Fig. 3(b) displays TGA

curves of neat PIL polymer and PIL-LiTFSI-IM(2o2)11TFSI electrolytes at different IM(2o2)11TFSI contents. The thermal decomposition temperatures (T_d) are measured at 5% weight loss. It appears clearly that the neat PIL polymer and PIL-LiTFSI-IM(2o2)11TFSI electrolyte samples all exhibit one-step thermal decomposition behaviors, which are different from those obtained for the mono-guanidinium based PIL electrolytes containing a guanidinium IL, it has been reported that mono-guanidinium based PIL electrolytes undergo two-step thermal decomposition.[26] Furthermore, the as-obtained neat PIL and PIL-based electrolyte samples have high thermal stability, and the decomposition temperatures of PIL, PVImN-90, PVImN-95 and PVImN-100 electrolytes are about 320℃, 326℃, 348℃ and 345℃, respectively.

Considering that ionic conductivity is one of the crucial properties for the electrochemical applications of electrolytes, the ionic conductivity as a function of temperature for PIL-LiTFSI-IM(2o2)11TFSI electrolyte samples is evaluated, and the corresponding results are presented in Fig. 4(a). It is apparent that ionic conductivity increases with the rise of temperature for the three investigated electrolyte samples, typically observed in polymer electrolytes. Faster migration of carrier ions and easier motion of PIL segments at higher temperature are responsible for this phenomenon.[36, 37] All of the electrolyte samples exhibit an Arrhenius behavior over the measured temperature range (25-90℃). It can also be observed that the ion conductivity depends on the PIL host and ionic liquid ratio. The more content of ionic liquid in the PIL-based electrolytes, the bigger local space for the motion of polymer segments, as well as the larger microscopically liquid environment for carrier ions, which thus improve ion-transporting property and consequently increase ion conductivity.[29, 38] This is consistent with DSC analysis from Fig. 3(a). The PVImN-100 sample exhibits an ionic conductivity of 0.46×10^{-4} S cm^{-1} and 1.37×10^{-4} S cm^{-1} at 25℃ and 40℃, respectively. This result suggests that the as-prepared PIL-based electrolytes could be used as promising electrolytes for lithium metal battery applications at low-medium temperatures. It should be noted that as the content of the IM(2o2)11TFSI ionic liquid is increased above 100 wt.%, the electrolyte membranes are sticky and difficult to handle.

Comparing the dicationic PIL (poly[VIm][TMEN][TFSI]) obtained in this work with the monocationic PIL, poly(1-ethyl-3-vinylimidazolium bis(trifluoromethanesulfonylimide)) (P(EtVIm-TFSI)), prepared in our previous

work,[30] obvious differences of IM(2o2)11TFSI ionic liquid incorporating ability can be observed. In the case of the monocationic PIL (P(EtVIm-TFSI)) as the polymer host, the maximum content of IM(2o2)11TFSI ionic liquid in the polymer electrolyte is about 65 wt.% (with respect to host), which is far below that in the dicationic PIL (poly[VIm][TMEN][TFSI]) host (95-100 wt.%). Considering that these two PILs are synthesized from the same homopolymer precursor (PVIm), the resulting dicationic PIL (poly[VIm][TMEN][TFSI]) and monocationic PIL (P(EtVIm-TFSI)) have the same degree of polymerization. Therefore, such differences of ionic liquid incorporating ability might be due to the different charge density and molecular structure between the dicationic PIL and monocationic PIL.

[Figure 4]

The electrochemical stability is also an important parameter to evaluate the potential applications of electrolytes. The results of linear sweep voltammograms of PIL-LiTFSI-IM(2o2)11TFSI electrolytes at 40℃ are shown in Fig. 4(b). It is clear that the current potential curves display almost no residual current between the cathodic and anodic decomposition voltages, indicating high purity of the PIL-based electrolytes, because the electrolyte system is electrochemically sensitive to impurities. In all cases, the cathodic and anodic decomposition voltages of PIL-based electrolytes are about 1.3 V(vs. Li/Li^+) and 4.5 V(vs. Li/Li^+), respectively. These results make the as-obtained PIL-based electrolytes promising candidates for LMBs.

[Figure 5]

In order to study the interfacial characteristics of PIL-based electrolyte/lithium metal, the charge-discharge cycling test of lithium symmetrical cells containing the PVImN-95 electrolyte were performed, and electrochemical impedance spectroscopy (EIS) before and after the cycling were also measured. Fig. 5 (a)-(b) show the voltage-time (V-t) profiles of lithium symmetrical cells underwent 100 charge-discharge cycles at 0.05 mA cm^{-2} and 0.1 mA cm^{-2} at 40℃, respectively. As expected, the voltage profiles do not exhibit huge random fluctuations and sudden voltage drop with continued cycling, indicating a stable SEI film formed on the lithium metal and no short-circuit effect occurred, as mentioned by

previous reports.[39-42] This finding confirms that the PVImN-95 electrolyte is efficient in promoting uniform Li electrodeposition on the lithium metal and possesses the advantage of suppressing the dendritic growth of lithium. In addition, it can be found that the overvoltage of the cell cycled at a current density of 0.05 mA cm^{-2} almost keeps a stable value, while a slight increase of overvoltage comes along with the cycling for the cell cycled at 0.1 mA cm^{-2}, which can be explained by that the polarization effect is more intensive at higher charge-discharge current density. Fig. 5 (c)-(d) show the EIS results before and after cycling test. The intercept of the impedance response with the real axis in the high frequency represents the electrolyte bulk resistance (R_b), and the diameter of the semicircle reflects the interfacial resistance (R_i) of PVImN-95 electrolyte/lithium metal.[43] It is obvious that R_b for the PVImN-95 electrolyte tested at 0.05 mA cm^{-2} and 0.1 mA cm^{-2} remains constant before and after the cycling, which indicates that the PVImN-95 electrolyte has excellent stability itself. Moreover, R_i for the PVImN-95 electrolyte just have a little changes after the cycling tests, implying good compatibility between the PVImN-95 electrolyte and lithium metal.

[Figure 6]

Fig. 6 depicts the cycling performance of Li/$LiFePO_4$ cells containing PIL-LiTFSI-IM(2o2)11TFSI electrolytes at 40℃. The cells with PVImN-100, PVImN-95 and PVImN-90 electrolytes all deliver initial discharge capacities of about 140mAh g^{-1} at a current rate of 0.1C. Also, in all cases, the discharge capacities steadily increase with ongoing cycling, which can be ascribed to the optimization of the electrode-electrolyte interfaces,[44] as commonly observed in monocationic PIL-based electrolytes.[28, 30] As for PVImN-100 and PVImN-95 electrolytes, the discharge capacities increase to approximately 160 mAh g^{-1} after 20 and 25 cycles, respectively, which is very close to the theoretical capacity (170 mAh g^{-1}), and then discharge capacities of 161.5 mAh g^{-1} and 161.1 mAh g^{-1} can still be remained after 50 cycles, respectively. This result show that the cells with as-prepared polymer electrolytes exhibit high discharge capacity and excellent capacity retention. Owing to that both the PVImN-95 electrolyte and the PVImN-100 electrolyte possess very similar cell performance, as well as the PVImN-95 electrolyte consumes lower ionic liquid amount, in the following, we select the PVImN-95 electrolyte as a representative of dicationic PIL-based electrolytes to be further evaluated in

$Li/LiFePO_4$ cells.

[Figure 7]

The performance of the $Li/LiFePO_4$ cell containing the PVImN-95 electrolyte at various temperatures (25℃, 30℃ and 40℃) is studied and the results are shown in Fig. 7. Fig. 7 (a) reports the initial charge-discharge curves of the $Li/PVImN\text{-}95/LiFePO_4$ cells. During the initial charge-discharge cycle at 25℃, 30℃ and 40℃, the cells deliver discharge capacities of 110.3 mAh g^{-1} with 83.9% coulombic efficiency, 124.4 mAh g^{-1} with 85.2% coulombic efficiency and 139.8 mAh g^{-1} with 87.3% coulombic efficiency, respectively. The irreversible capacity loss in the first cycle is attributed to the formation of protective solid electrolyte interface (SEI) film at the lithium anode.[45, 46] In the case of the cells operating at 30℃ and 40℃, the initial charge-discharge profiles show a flat plateau at 3.5 V (vs. Li/Li^+) and 3.4-3.3 V (vs. Li/Li^+), which is a typical feature of $Li/LiFePO_4$ batteries.[25, 30, 37] It can also be found that the voltage polarization effect between the charge and discharge plateaus becomes more intensive when the temperature decreases from 40℃ to 25℃, suggesting an increase in the internal resistance of the lithium cell. Fig. 7 (b) and (c) illustrate the cycle-number dependence of discharge capacity and coulombic efficiency of $Li/PVImN\text{-}95/LiFePO_4$ cells, respectively. As clearly evidenced from Fig. 7 (b) , the discharge capacity increase with rising the operational temperature, because the ion transfer in the PIL-based electrolyte becomes faster, as well as the extraction and insertion of lithium ion into the $LiFePO_4$ electrode become easier at higher temperature.[47] As mentioned above, the $Li/PVImN\text{-}95/LiFePO_4$ cell tested at 40℃ exhibits a high discharge capacity of 161.1 mAh g^{-1} (94.8% of the theoretical value) after 50 cycles. When the operational temperature reduces to 30℃, the cell is capable to achieve a discharge capacity of approximately 140 mAh g^{-1} after initial 10 cycles, and still maintain a discharge capacity of 141.7 mAh g^{-1} (83.4% of the theoretical value) after 50 cycles，indicating satisfactory discharge capacity and excellent cycling performance at 30℃ , which would meet the energy density requirement for battery application. As the operational temperature further declines to 25℃, a stable discharge capacity of about 120 mAh g^{-1} (70.6% the theoretical value) can still be obtained after 50 cycles. In addition, from Fig. 7 (c), we can observe that the coulombic efficiency approaches above 99% after several cycles for the cells,

which reflects highly reversible charge-discharge ability. Such findings reveal that the dicationic PIL-based electrolytes prepared in this work exhibit cell performances that are comparable and, in some cases, even better than those for PIL-based electrolytes reported in the recent literatures.[25, 28-30] The rate performance of the Li/$LiFePO_4$ cell containing PVImN-95 electrolyte is also preliminarily investigated to exploit the potential application in high-power lithium batteries, and the results are shown in Fig. 7(d). It can be seen that increasing the discharge current rate leads to the drop in the discharge plateau voltage, which is due to an enhancement of the cell polarization. In the cases of 0.1C and 0.5C rates, the discharge processes are revealed by 3.4 V (vs. Li/Li^+) and 3.2-3.1 V (vs. Li/Li^+), respectively. While the rate is up to 1.0C, the flat plateau is not clearly visible. This trend is similar to those reported in previous works.[25, 47] Despite all that, under these conditions, the cell still show an acceptable rate capability with stable discharge capacities of about 160 mAh g^{-1} (0.1C), 128.8 mAh g^{-1} (0.5C) and 83 mAh g^{-1} (1.0C) in this system.

4.Conclusions

In summary, an imidazolium-tetraalkylammonium-based dicationic polymerized ionic liquid (PIL), poly(N,N,N-trimethyl-N-(1-vinlyimidazolium-3-ethyl)-ammonium bis(trifluoromethanesulfonyl) -imide) has been successfully synthesized and characterized. Moreover, the ternary gel polymer electrolytes based on the as-obtained dicationic PIL as the polymer host in combination with 1,2-dimethyl-3-ethoxyethyl imidazolium bis(trifluoromethanesulfonyl) imide ionic liquid (IM(2o2)11TFSI) and LiTFSI salt in different weight ratios have been prepared, and their properties have been investigated. The dicationic PIL-based electrolytes exhibit low glass-transition temperatures, high thermal and electrochemical stability, acceptable ion conductivity, as well as satisfactory interfacial stability with metallic lithium. Particularly, the Li/$LiFePO_4$ cells with the ternary gel polymer electrolytes are capable of delivering discharge capacities of about 160 mAh g^{-1}, 140 mAh g^{-1} and 120 mAh g^{-1} at 0.1C rate at 40℃, 30℃ and 25℃, respectively, and show good capacity retention. In addition, the cells also present acceptable rate capability. Such impressive results, especially excellent battery performance at low-medium temperatures make the dicationic PIL-based electrolytes prepared in this work as promising electrolytes for highly safe lithium metal batteries.

Acknowledgements

The authors are indebted to the National Natural Science Foundation of China (Grants No. 21373136) and Hitachi Chemical Co. Ltd. We thank the Instrumental Analysis Center of Shanghai Jiao Tong University for Materials Characterization.

Notes

a. School of Chemistry and Chemical Engineering, Shanghai Jiao Tong University, Shanghai 200240, PR China

b. Department of Chemistry and Chemical Engineering, Faculty of Engineering, Yamagata University,Yamagata 992-8510, Japan

c. Hirano Institute for Materials Innovation, Shanghai Jiao Tong University, Shanghai 200240, PR China

*Corresponding author: Tel. +86 21 54748917; Fax:+86 21 54741297

E-mail: zhengxizhang@sjtu.edu.cn(Z.X. Zhang); liyangce@sjtu.edu.cn(L.Yang)

References

1. J. M. Tarascon and M. Armand, *Nature*, 2001, **414**, 359-367.
2. I. Yoshimatsu, T. Hirai and J. Yamaki, *J. Elctrochem. Soc.*, 1988, **135**, 2422-2427.
3. M. Armand and J. M. Tarascon, *Nature*, 2008, **451**, 652-657.
4. J. B. Goodenough and Y. Kim, *Chemistry of Materials*, 2010, **22**, 587-603.
5. S. Ferrari, E. Quartarone, P. Mustarelli, A. Magistris, M. Fagnoni, S. Protti, C. Gerbaldi and A. Spinella, *J Power Sources*, 2010, **195**, 559-566.
6. P. Isken, M. Winter, S. Passerini and A. Lex-Balducci, *J Power Sources*, 2013, **225**, 157-162.
7. T. Matsui and K. Takeyama, *ELectrochimica Acta*, 1995, **40**, 2165-2169.
8. T. Osaka, T. Homma, T. Momma and H. Yarimizu, *J Electroanal Chem*, 1997, **421**, 153-156.
9. T. Tatsuma, M. Taguchi and N. Oyama, *Electrochimica Acta*, 2001, **46**, 1201-1205.
10. T. Tatsuma, M. Taguchi, M. Iwaku, T. Sotomura and N. Oyama, *J Electroanal Chem*, 1999, **472**, 142-146.
11. A. Manuel Stephan, *European Polymer Journal*, 2006, **42**, 21-42.
12. J. W. Fergus, *J Power Sources*, 2010, **195**, 4554-4569.
13. E. Quartarone and P. Mustarelli, *Chemical Society reviews*, 2011, **40**, 2525-2540.

14. C. Gerbaldi, J. R. Nair, S. Ferrari, A. Chiappone, G. Meligrana, S. Zanarini, P. Mustarelli, N. Penazzi and R. Bongiovanni, *Journal of Membrane Science*, 2012, **423-424**, 459-467.
15. J. Yuan, D. Mecerreyes and M. Antonietti, *Progress in Polymer Science*, 2013, **38**, 1009-1036.
16. A.-L. Pont, R. Marcilla, I. De Meatza, H. Grande and D. Mecerreyes, *J Power Sources*, 2009, **188**, 558-563.
17. A. Balducci, S. S. Jeong, G. T. Kim, S. Passerini, M. Winter, M. Schmuck, G. B. Appetecchi, R. Marcilla, D. Mecerreyes, V. Barsukov, V. Khomenko, I. Cantero, I. De Meatza, M. Holzapfel and N. Tran, *J Power Sources*, 2011, **196**, 9719-9730.
18. H. Ohno and K. Ito, *Chem Lett*, 1998, 751-752.
19. M. Yoshizawa, W. Ogihara and H. Ohno, *Polym Advan Technol*, 2002, **13**, 589-594.
20. R. Marcilla, J. A. Blazquez, J. Rodriguez, J. A. Pomposo and D. Mecerreyes, *J Polym Sci Pol Chem*, 2004, **42**, 208-212.
21. H. Chen, J.-H. Choi, D. Salas-de la Cruz, K. I. Winey and Y. A. Elabd, *Macromolecules*, 2009, **42**, 4809-4816.
22. M. D. Green, D. Salas-de la Cruz, Y. Ye, J. M. Layman, Y. A. Elabd, K. I. Winey and T. E. Long, *Macromolecular Chemistry and Physics*, 2011, **212**, 2522-2528.
23. M. Döbbelin, I. Azcune, M. Bedu, A. Ruiz de Luzuriaga, A. Genua, V. Jovanovski, G. Cabañero and I. Odriozola, *Chemistry of Materials*, 2012, **24**, 1583-1590.
24. J. Bandomir, A. Schulz, S. Taguchi, L. Schmitt, H. Ohno, K. Sternberg, K.-P. Schmitz and U. Kragl, *Macromolecular Chemistry and Physics*, 2014, **215**, 716-724.
25. G. B. Appetecchi, G. T. Kim, M. Montanino, M. Carewska, R. Marcilla, D. Mecerreyes and I. De Meatza, *J Power Sources*, 2010, **195**, 3668-3675.
26. M. Li, L. Yang, S. Fang, S. Dong, S.-i. Hirano and K. Tachibana, *J Power Sources*, 2011, **196**, 8662-8668.
27. M. Li, L. Yang, S. Fang, S. Dong, S.-i. Hirano and K. Tachibana, *Polymer International*, 2012, **61**, 259-264.
28. M. Li, B. Yang, L. Wang, Y. Zhang, Z. Zhang, S. Fang and Z. Zhang, *Journal of Membrane Science*, 2013, **447**, 222-227.
29. M. Li, L. Wang, B. Yang, T. Du and Y. Zhang, *Electrochimica Acta*, 2014, **123**, 296-302.
30. K. Yin, Z. Zhang, L. Yang and S.-I. Hirano, *J Power Sources*, 2014, **258**, 150-154.
31. Y. Jin, S. Fang, M. Chai, L. Yang and S.-i. Hirano, *Industrial & Engineering Chemistry Research*, 2012, **51**, 11011-11020.
32. J. Brandrup, E. H. Immergut and E. A. Grulke, Polymer HandBook, 4th ed.; *Wiley*: New York, 1999.
33. X. Chen, J. Zhao, J. Zhang, L. Qiu, D. Xu, H. Zhang, X. Han, B. Sun, G. Fu, Y. Zhang and F. Yan, *Journal of Materials Chemistry*, 2012, **22**, 18018-18024.
34. Ľ. Jankovič, J. Madejová, P. Komadel, D. Jochec-Mošková and I. Chodák, *Applied Clay Science*, 2011, **51**, 438-444.
35. E. H. Cha, D. R. Macfarlane, M. Forsyth and C. W. Lee, *Electrochimica Acta*, 2004, **50**, 335-338.
36. Z. Cui, Y. Xu, L. Zhu, J. Wang, Z. Xi and B. Zhu, *Journal of Membrane Science*, 2008, **325**, 957-963.
37. N. H. Idris, M. M. Rahman, J.-Z. Wang and H.-K. Liu, *J Power Sources*, 2012, **201**, 294-300.
38. C. Liao, X.-G. Sun and S. Dai, *Electrochimica Acta*, 2013, **87**, 889-894.
39. Y. Lu, S. K. Das, S. S. Moganty and L. A. Archer, *Advanced materials*, 2012, **24**, 4430-4435.
40. M. Rosso, C. Brissot, A. Teyssot, M. Dollé, L. Sannier, J.-M. Tarascon, R. Bouchet and S. Lascaud, *Electrochimica Acta*, 2006, **51**, 5334-5340.
41. Y. Lu, K. Korf, Y. Kambe, Z. Tu and L. A. Archer, *Angewandte Chemie*, 2014, **53**, 488-492.
42. H. Yoon, G. H. Lane, Y. Shekibi, P. C. Howlett, M. Forsyth, A. S. Best and D. R. MacFarlane, *Energy & Environmental Science*, 2013, **6**, 979-986.
43. A. Fernicola, F. Croce, B. Scrosati, T. Watanabe and H. Ohno, *J Power Sources*, 2007, **174**, 342-348.
44. J.-H. Shin, W. A. Henderson and S. Passerini, *Journal of The Electrochemical Society*, 2005, **152(5)**, A978-A983.
45. E. Peled, D. Golodnitsky and G. Ardel, *Journal of the Electrochemical Society*, 1997, **144**, L208-L210.
46. B. W. Zewde, S. Admassie, J. Zimmermann, C. S. Isfort, B. Scrosati and J. Hassoun, *ChemSusChem*, 2013, **6**, 1400-1405.
47. F. Wu, G. Tan, R. Chen, L. Li, J. Xiang and Y. Zheng, *Advanced materials*, 2011, **23**, 5081-5085.

Tables and Figures

Table 1 Composition of gel polymer electrolytes.

Sample	Weight composition (wt. %)		
	poly[VIm][TMEN][TFSI] (host)	IM(2o2)11TFSI (ionic liquid)	LiTFSI (Li salt)
PVImN-90	100	90	30
PVImN-95	100	95	30
PVImN-100	100	100	30

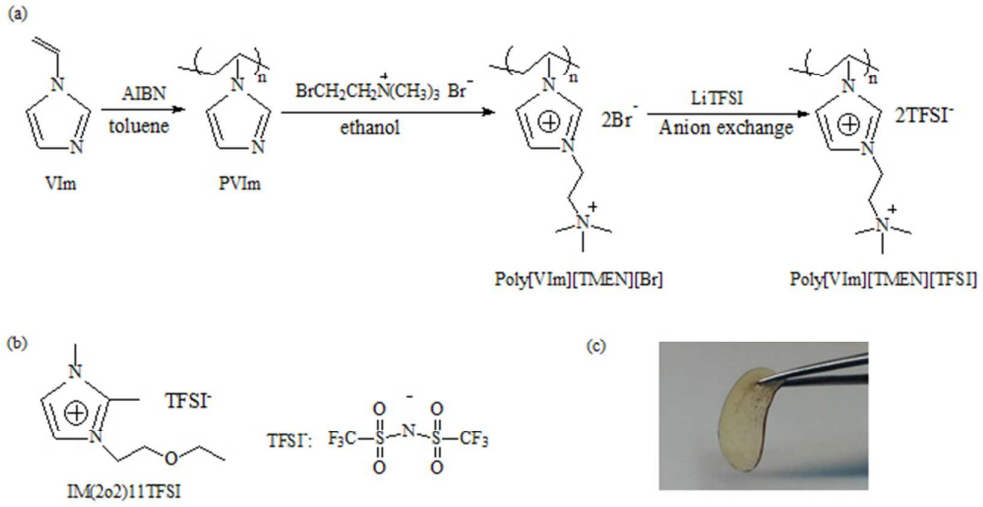

Fig. 1. (a): synthetic route of the imidazolium-tetraalkylammonium-based PIL. (b): structure of IM(2o2)11TFSI. (c): picture of a PIL-LiTFSI-IM(2o2)11TFSI electrolyte (PVImN-95 sample).

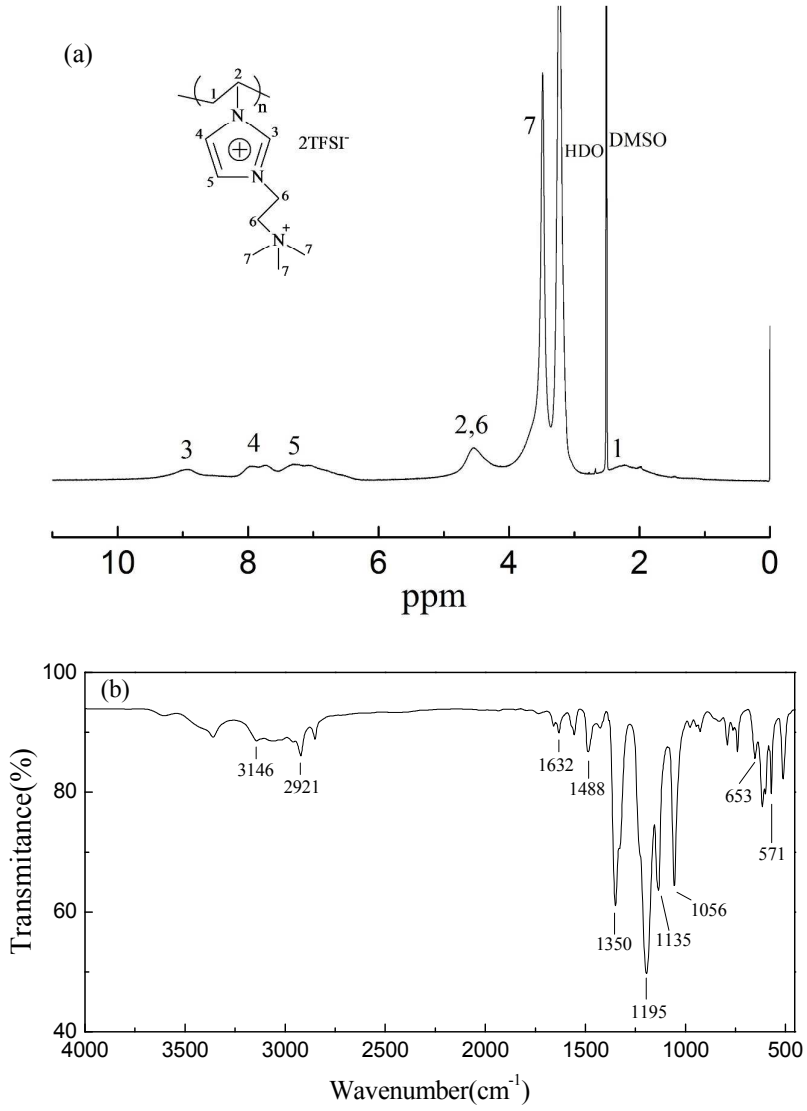

Fig. 2. (a) ^{1}H NMR spectrum and (b) FT-IR spectrum of the PIL (poly[VIm][TMEN][TFSI]).

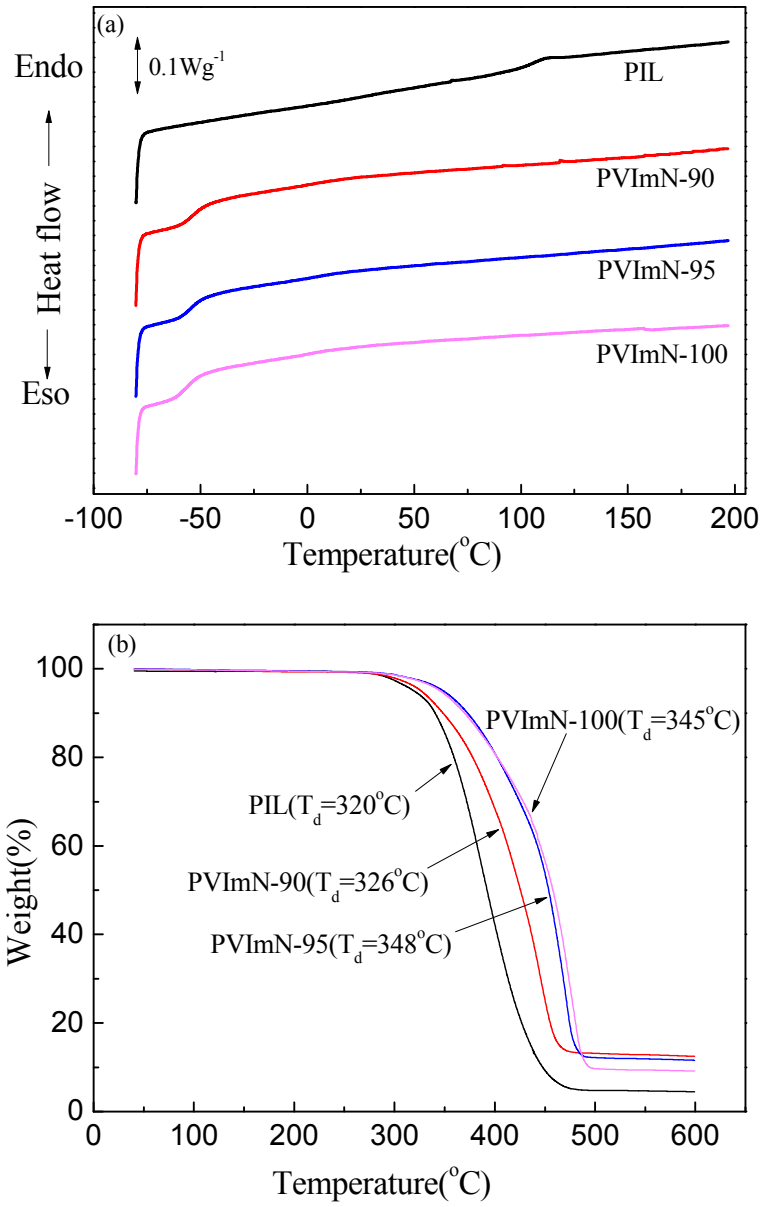

Fig. 3. (a) DSC curves and (b) TGA curves of neat PIL polymer and PIL-LiTFSI-IM(2o2)11TFSI electrolyte samples with different IM(2o2)11TFSI contents. Scan rate: 10□ min^{-1}.

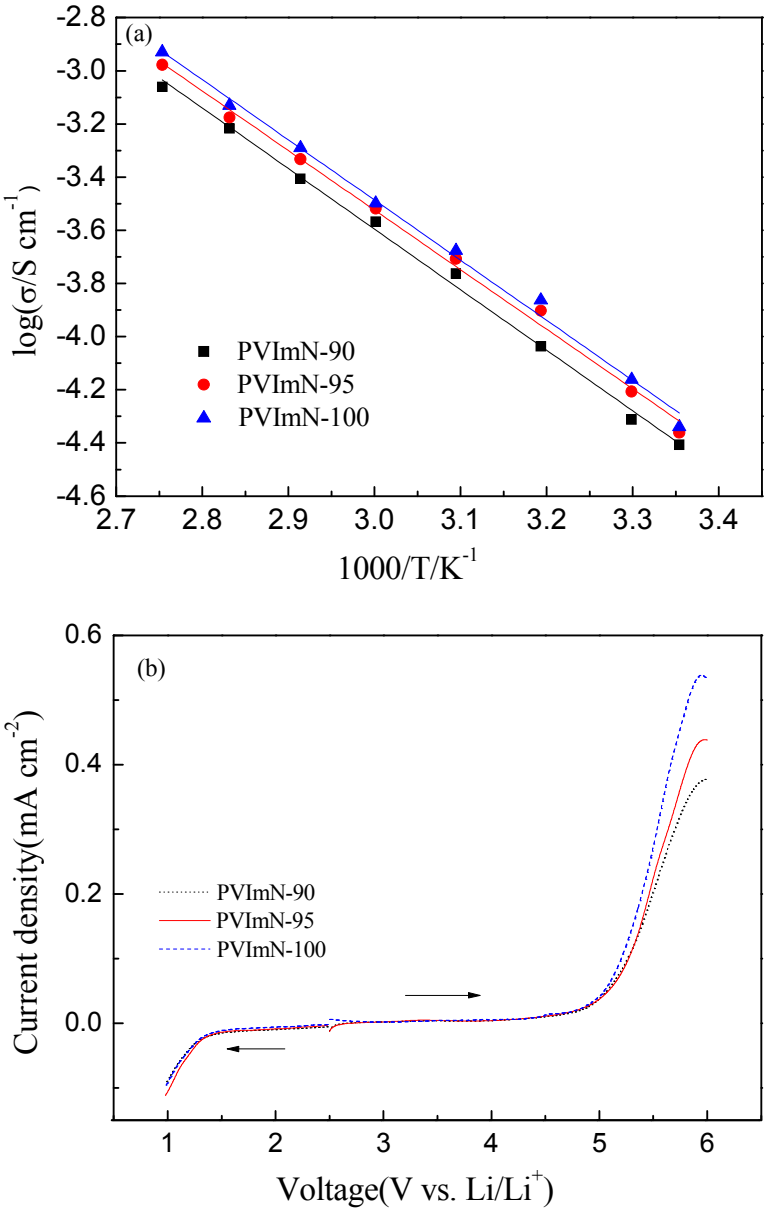

Fig. 4. (a) Temperature dependence of ionic conductivity for PIL-LiTFSI-IM(2o2)11TFSI electrolyte samples with different IM(2o2)11TFSI contents. (b) Linear sweep voltammograms of the PIL-LiTFSI-IM(2o2)11TFSI electrolytes at 40℃(SS/ PIL-based electrolyte/Li cells, working electrode: SS, counter and reference electrodes: lithium metal, scan rate: 10 mv s^{-1}).

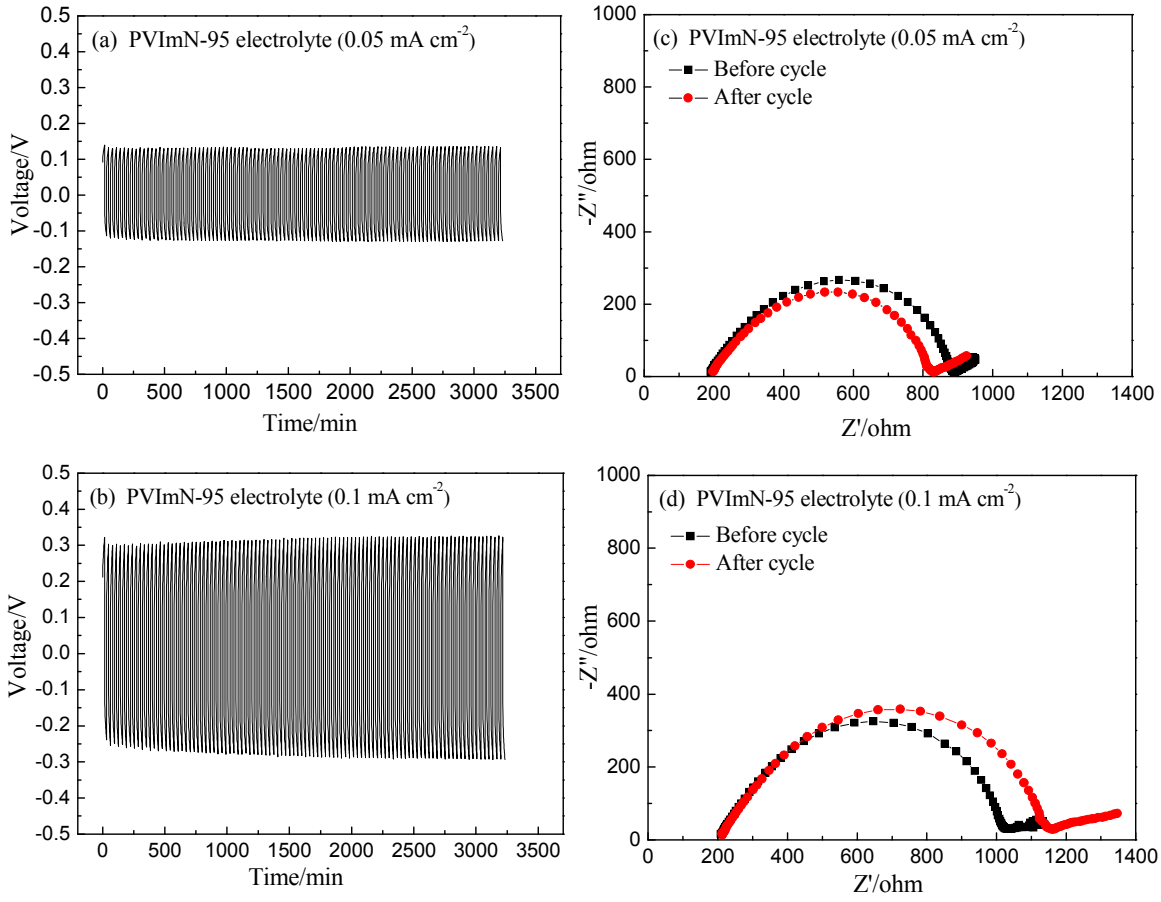

Fig. 5. Li symmetrical cell cycling and EIS results of a cell containing PVImN-95 electrolyte: 16 mm Li disc, constant current for 16 min, 100 cycles at 40℃; (a) and (c) 0.05 mA cm^{-2}, (b) and (d) 0.1 mA cm^{-2}.

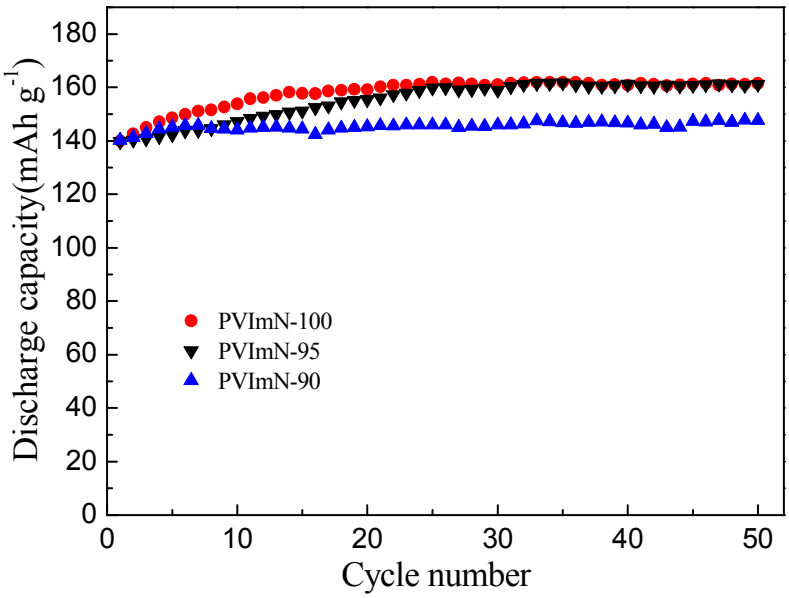

Fig. 6. Cycling performance of Li/$LiFePO_4$ cells containing PIL-LiTFSI-IM(2o2)11TFSI electrolyte samples at 40℃ (2.5-4.0 V), charge-discharge current rate is 0.1C.

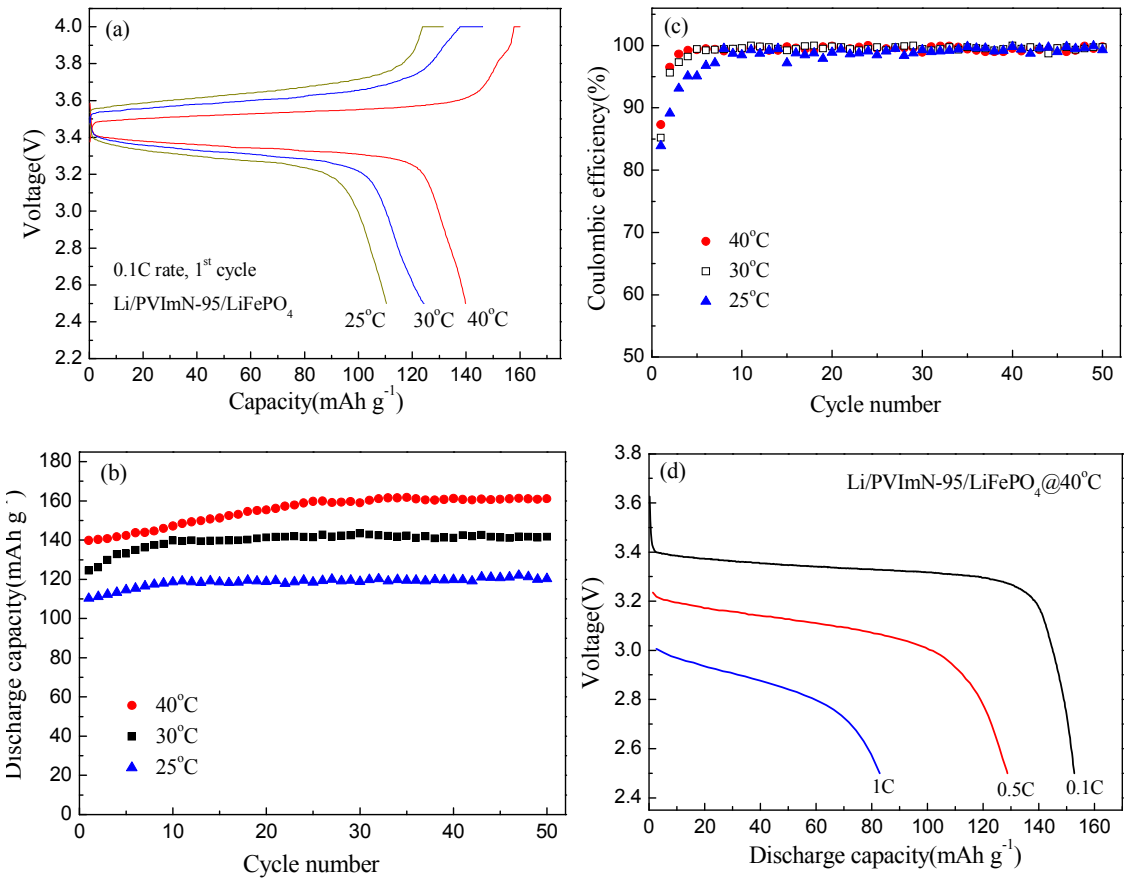

Fig. 7. Cell Performance of Li/ PVImN-95/ $LiFePO_4$ cells. (a) Charge-discharge curves for initial cycles at three temperatures, (b) cycling performance of cells at 0.1C as a function of temperatures , (c) cycle-number dependence of coulombic efficiency and (d) discharge curves of selected half cycles at various current rates at 40℃, charging at 0.1C rate and discharging at various current rates.